biomolecules

MDPI

Article

Physiological Aging Limits the Antioxidant Effects of Fenofibrate in the Rat Heart

Agata Wrońska [1,*], Jacek Kieżun [2] and Zbigniew Kmieć [2]

[1] Department of Histology, Faculty of Medicine, Medical University of Gdańsk, 80-211 Gdańsk, Poland
[2] Department of Anatomy and Histology, School of Medicine, University of Warmia and Mazury in Olsztyn, 10-082 Olsztyn, Poland; jacek.kiezun@uwm.edu.pl (J.K.); zbigniew.kmiec@uwm.edu.pl (Z.K.)
* Correspondence: agata.wronska@gumed.edu.pl

Abstract

The lipid-lowering drug fenofibrate (FF) can mitigate oxidative stress in various pathological settings, including cardioprotection. We examined whether this effect is retained in the aged heart. Cardiac tissue from young and old male rats treated for 30 days with 0.1% or 0.5% FF in chow was analyzed for oxidative stress markers and antioxidant gene and protein expression. Basal levels of the oxidative DNA damage marker 8-OH-dG were similar in young and old hearts, while the lipid peroxidation product 4-hydroxynonenal was elevated in old controls. FF did not significantly affect 8-OH-dG in young hearts, but both doses elevated its levels in old hearts. In young rats, 0.5% FF induced Nrf2 and downstream antioxidant effectors, including *Nqo1*, mitochondrial *Txn2*, and *Prdx5*, while 0.1% FF stimulated *Nqo1* expression and Ho1 immunoreactivity. Conversely, aged myocardium exhibited a blunted response, as FF failed to induce Nrf2 or its target genes and did not stimulate mitochondrial antioxidant remodeling. FF also increased Angpt1 but not eNOS expression in young animals. In conclusion, physiological aging limits the cardiac antioxidant effects of fenofibrate. The lack of Nrf2 induction and the potential for enhanced DNA damage in aged hearts suggest that FF's cardioprotective benefits may not translate to the elderly.

Keywords: aging; fenofibrate; heart; oxidative stress; antioxidant response

1. Introduction

The aging process entails molecular changes that affect multiple organ systems, including the cardiovascular system. Older age, in addition to hypertension, hyperlipidemia, obesity, and diabetes, is an independent risk factor for cardiovascular diseases (CVDs), still a leading cause of mortality and morbidity despite improvements in medical care [1,2]. CVD risk can be reduced with lipid-lowering drugs such as fenofibrate (FF), indicated for mixed-type dyslipidemia and hypertriglyceridemia, particularly in patients with atherogenic dyslipidemia or those intolerant to statins [3]. Several large-scale human studies demonstrated cardioprotective effects of FF, including reduced risk of major cardiovascular events, microvascular complications, and fewer heart failure-related hospitalizations in sub-populations of type 2-diabetic (T2D) patients [4–6]. In rodents, FF ameliorated pathological changes in acute and chronic cardiac injury models, including diabetes [7,8], myocardial ischemia/reperfusion injury [9,10], and hypertension [11–14]. However, little is known about the cardioprotective potential of FF in physiological aging.

Through its agonism of peroxisome proliferator-activated receptor alpha (PPARα), FF activates cellular responses involving increased lipid oxidation, downregulation of inflammatory pathways, and attenuation of oxidative stress [15]. In young rats treated for two

Check for updates

Academic Editor: Jian Yao

Received: 14 October 2026
Revised: 21 November 2026
Accepted: 24 November 2026
Published: 26 November 2026

Copyright: © 2026 by the authors. Licensee MDPI, Basel, Switzerland. This article is an open access article distributed under the terms and conditions of the Creative Commons Attribution (CC BY) license.

weeks with FF and subjected to myocardial infarction, FF reduced cardiac malondialdehyde levels and increased total antioxidant capacity by upregulating Cu/Zn- and Mn-superoxide dismutases and catalase [16]. Similar effects were observed in primary cultures of neonatal rat cardiomyocytes subjected to hypoxia/reoxygenation or high-glucose stress [17]. In streptozotocin-induced diabetic mice, FF mitigated cardiac oxidative damage, as measured by levels of the biomarker nitrotyrosine [18]. However, these findings predominantly originate from cellular models or pathological models established in young animals, leaving the influence of physiological aging on the cardiac response to FF largely unexplored. This knowledge gap is particularly relevant given that aging is associated with progressive mitochondrial dysfunction, reactive oxygen species (ROS) accumulation, and declining antioxidant defenses [19]. Importantly, this age-associated oxidative stress may develop even in the absence of overt clinical pathology. Therefore, an additional question is whether FF can safely counteract the elevated basal oxidative burden characteristic of physiological aging, or whether age-related changes may predispose to adverse responses to FF action. This question is of translational relevance, as older individuals frequently present with mild age-associated dyslipidemia [20], which may provide a rationale for considering fibrate therapy. However, the potential benefits of FF in this context must be weighed against the possibility that physiological aging alters cardiac tissue susceptibility to its pharmacological effects. Thus, the influence of physiological aging on FF-mediated cardiac antioxidant mechanisms remains an important unresolved question.

Although aging is frequently associated with alterations in drug pharmacokinetics [21], its potential impact on tissue-level pharmacological responses is insufficiently investigated. Preclinical studies predominantly employ young adult animals, potentially overlooking age-dependent modifications in drug efficacy and tissue responses. Our previous studies using a rat model of physiological aging demonstrated that FF induced more pronounced structural and ultra-structural changes in the liver of old as compared to young rats [22], while in adipose tissue it induced oxidative metabolism-related targets mostly in young animals [23]. In the kidney, FF stimulated some antioxidant genes only in young rats, while high-dose FF exacerbated oxidative damage in aged animals, as demonstrated by increased 4-hydroxynonenal (4-HNE) immunoreactivity [24]. Moreover, high-dose FF promoted collagen deposition, lipid accumulation in cardiomyocytes, and upregulation of hypertrophy-associated markers in hearts of old rats [25]. These observations suggest that physiological aging may modify tissue responses to pharmacological stimulation with FF.

The present study aimed to investigate how physiological aging per se modifies the cardiac antioxidant response to FF by comparing young and old male rats. Our findings demonstrate that physiological aging limits the cardiac antioxidant response to FF, highlighting age as a potential determinant of the drug's cardiac effects.

2. Materials and Methods

2.1. Animals and Experimental Procedures

The study was conducted on male Wistar-Han rats maintained under standard laboratory conditions at the Academic Animal Experimental Centre of the Medical University of Gdańsk, Gdańsk, Poland. All procedures were approved by the Local Ethical Committee in Bydgoszcz, Poland (protocol No. 41/2017, approved on 27 July 2017, for treatment of old rats with 0.5% FF; protocol No. 58/2017, approved on 23 November 2017, for treatment of young rats with 0.5% FF; protocol No. 40/2018, approved on 16 October 2018, for treatment of old rats with 0.1% FF; protocol No. 5/2019, approved on 20 February 2019, for treatment of young rats with 0.1% FF). The experiment was conducted in accordance with institutional and European regulations on animal research.

Following two weeks of acclimation, young adult (4 months) and aged rats (24 months) were subdivided into control (fed a standard laboratory chow: Labofeed H, Wytwórnia Pasz Morawski, Kcynia, Poland) and FF-treated groups. To minimize stress during handling procedures, FF (Glentham Life Sciences, Corsham, UK) was administered in a form premixed into chow during pelleting, at 0.1% or 0.5% (*w*/*w*). The biological tissue samples analyzed in this study were harvested from the same animal cohorts previously examined for other organ- or tissue-specific effects [22–25]. The 0.5% FF dose, corresponding to approx. 100 mg daily intake or 260 mg/kg body weight (bw) in young and 210 mg/kg bw in old rats [24], caused mild hepatotoxicity [22]; therefore, a separate cohort was treated with 0.1% FF, amounting to approx. 52 mg/kg bw in young and 42 mg/kg bw in old rats. As no statistical differences were observed in any of the measured parameters between control animals from the two experiments, their data were analyzed together.

After 30 days of the experiment, animals were fasted overnight, anesthetized with 5% isoflurane, and euthanized by exsanguination via cardiac puncture. Cardiac muscle samples were rapidly excised, rinsed in ice-cold phosphate-buffered saline, and dissected according to a standardized protocol applied across all experimental groups. For molecular analyses (qPCR, Western blotting, and ELISA), the cardiac apex was halved, immediately frozen in liquid nitrogen, and stored at −80 °C in separate vials for RNA isolation (up to 6 months, followed by storage of cDNA samples until analyses) and preparation of protein lysates (storage up to 4 years). Freeze–thaw cycles were strictly avoided. For immunohistochemical (IHC) examinations, a transverse section through both ventricles was made at the mid-papillary level, fixed in 2–3 changes of neutralized 4% paraformaldehyde, and processed for paraffin embedding within several months.

Profiles of the changes in body weight, food consumption, and estimated daily intake of FF have been reported previously [22].

2.2. Evaluation of Oxidative DNA Damage

Oxidative DNA damage was assessed using a competitive ELISA kit for 8-hydroxydeoxyguanosine (8-OHdG; #E-EL-0028, Elabscience, Houston, TX, USA), following the manufacturer's protocol. Cardiac lysates (RIPA Lysis Buffer, EURx, Gdańsk, Poland) were analyzed at a 1:100 dilution. Absorbance was measured at 450 nm using an Epoch microplate reader (Agilent Technologies, Santa Clara, CA, USA).

2.3. Immunohistochemical Analyses

Immunohistochemical (IHC) staining was performed according to the protocol described by Kiezun et al. [26], with modifications. Antigen retrieval was performed by microwaving sections for 6 min in pH 6.0 Retrieval Solution (Leica Microsystems, Wetzlar, Germany), followed by blocking endogenous peroxidase with 3% hydrogen peroxide in methanol for 10 min. Sections were incubated with 2.5% normal horse serum (Vector Laboratories, Birmingham, CA, USA) for 30 min at room temperature and then overnight at 4 °C with rabbit polyclonal antibodies against 4-hydroxynonenal (4-HNE; #bs-6313R, Bioss, Woburn, MA, USA) or heme oxygenase 1 (Ho1; #bsm-60751R, Bioss), diluted 1:200 in PBS. Staining specificity was verified by omitting the primary antibody and substituting normal rabbit serum. Sections were incubated with ImmPRESS Universal Anti-Rabbit Ig reagent (Vector Laboratories, Birmingham, CA, USA) for 30 min, and immunoreactivity was detected using Liquid DAB+ Substrate Chromogen System (Dako, Carpinteria, CA, USA). Sections were counterstained with hematoxylin (Sigma-Aldrich, Merck KGaA, St. Louis, MO, USA).

Images were acquired using an SC-50 camera mounted on an Olympus CX31 microscope (Olympus Corp., Tokyo, Japan). 4-HNE immunoreactivity was quantified using

the Count and Measure tool in cellSens Dimension 4.1 software (Olympus Corp.) on RGB-separated images with optimized thresholds, analyzing at least 8 ROIs per slide from 3 to 8 animals/group. Ho1 immunoreactivity was quantified using a neural network in cellSens Dimension 4.1, trained to distinguish erythrocytes from cardiomyocytes; only cardiomyocytic immunoreactivity was analyzed. Measurements from all ROIs of a given tissue section were averaged to yield a single composite mean value per animal. Statistical comparisons were performed using these animal-level biological replicates.

2.4. Immunoblotting

Cardiac tissue lysates (approx. 40 µg total protein/sample) were separated on 12% SDS–polyacrylamide gels and transferred onto PVDF membranes (Bio-Rad, Hercules, CA, USA). Membranes were blocked for 1 h in 5% BSA (#A3294, Sigma-Aldrich, Merck KGaA, St. Louis, MO, USA) and incubated overnight at 4 °C with antibodies targeting Nrf2 (#D1Z9C, Cell Signaling Technology, Danvers, MA, USA), Sesn2 (#10795-1-AP, Proteintech, Rosemont, IL, USA), Ho1 (#E3F4S, Cell Signaling Technology), Nqo1 (#D6H3A, Cell Signaling Technology), eNOS (#D9A5L, Cell Signaling Technology), and Angpt1 (#bs-0800R, Bioss). Gapdh (#AB2302, Sigma-Aldrich, Merck KGaA, St. Louis, MO, USA) served as the loading control. After washing, membranes were incubated for 1 h with Alexa Fluor®-conjugated anti-rabbit secondary antibodies (#111-625-144, Jackson ImmunoResearch, West Grove, PA, USA). Signals were visualized using the Odyssey® CLx Imaging System (LI-COR® Biosciences, Lincoln, NE, USA) and quantified by densitometry with ImageQuant™ TL 10.0 software (Cytiva Europe GmbH, Freiburg im Breisgau, Germany).

2.5. Reverse Transcription and Quantitative Real-Time PCR

Total RNA was extracted from cardiac tissue homogenates using the Total RNA Mini Plus kit (A&A Biotechnology, Gdynia, Poland), followed by reverse transcription using the smART First Strand cDNA Synthesis Kit (EURx, Gdańsk, Poland). qPCR was carried out using 5× diluted cDNA as a template, SybrGreen qPCR Master Mix (EURx), and 0.25 µM each of gene-specific sense and antisense primers (Sigma-Aldrich). Primer sequences, designed using Primer-BLAST (based on Primer3 (version 2.5.0) and BLAST tools; NCBI, Bethesda, MD, USA), are presented in Table 1. Amplification specificity was confirmed by dynamic melting curve analysis. Relative gene expression was calculated using the comparative $2^{-\Delta\Delta CT}$ method, normalized to the geometric mean of *Arbp* and *Rplp1*.

Table 1. List of primers.

Gene Symbol	Gene Name	Forward and Reverse Primer Sequences
Arbp [1]	60S acidic ribosomal protein P0	CTCAGTGCCTCACTCCATCA GGGGCTTAGTCGAAGAGACC
Gpx4	Glutathione peroxidase 4	CTGTGTAAATGGGGACGATG AGAGATAGCACGGCAGGT
Ho1	Heme oxygenase 1	TCAGAAGGGTCAGGTGTCCA GGGTTCTGCTTGTTTCGCTC
Nqo1	NAD(P)H quinone dehydrogenase 1	TTCGCCTACACGTATGCCAC CAGAGAGTACATGGAGCCGC
Prdx1	Peroxiredoxin 1	ACACACCCAAGAAACAAGG CTCATCCACAGAGCGG
Prdx2	Peroxiredoxin 2	GGACTCTCAGTTCACCC GGACACCCTTGGCATC

Table 1. *Cont.*

Gene Symbol	Gene Name	Forward and Reverse Primer Sequences
Prdx3	Peroxiredoxin 3	TATCGTGGCTCTTGCGTTC ACTTTGCTTGGGGACAGG
Prdx5	Peroxiredoxin 5	GCTGAGGTTTTGCGTCCT CACTGAGGGAATGGTGTCTC
Rplp1 [1]	Large ribosomal subunit protein P1	AAGCAGCTGGTGTCAATGTTG CAGCCCCTACATTGCAGATGA
Srxn1	Sulfiredoxin 1	CCCAAGGCGGTGACTACTAC GACCTCACGAGCTTGGCAG
Txn1	Thioredoxin 1	GCCCTTCTTTCATTCCCTCTGT CCCCAACCTTTTGACCCTTTT
Txn2	Thioredoxin 2	GGTCTAACTGGAACACCCA GCTACCATCTTCTCTAACCGAG

[1] Housekeeping gene.

2.6. Statistical Analyses

Data were analyzed using GraphPad Prism v.6 (GraphPad Software, San Diego, CA, USA). Normality of distribution was assessed with the Shapiro–Wilk test, and homogeneity of variances was assessed using the Brown–Forsythe test. Statistical outliers were identified using the ROUT method (Q = 1%) and excluded prior to analysis ($n = 3$). For normally distributed datasets, data were analyzed using one-way ANOVA with Tukey's post hoc tests for pairwise comparisons. For non-normally distributed datasets, a Kruskal–Wallis test followed by Dunn's post hoc test was applied. To detect Age × Treatment interaction, a two-way factorial ANOVA with Type III sums of squares, followed by Tukey–Kramer HSD post hoc comparisons, was performed. Results are presented as means + SEM, with $p < 0.05$ considered statistically significant. Differences between experimental groups are indicated by asterisks: * $p < 0.05$, ** $p < 0.01$, *** $p < 0.001$.

3. Results

3.1. Fenofibrate-Induced Changes in Blood Lipid Levels

The hypolipidemic effect of FF was assessed based on concentrations of triglycerides and total cholesterol in blood serum (Table 2) [22]. Aging was associated with elevated concentrations of triglycerides and total cholesterol. 0.1% FF decreased cholesterol levels only in young rats, whereas 0.5% FF decreased triglyceride concentration only in old rats [22].

Table 2. Lipid concentrations in blood serum.

	yC	y.1	y.5	oC	o.1	o.5
Est. FF intake (mg/kg/day)	—	52	260	—	42	210
TG (mg/dL)	53.18 ± 5.50	40.44 ± 5.13	46.50 ± 4.18	114.5 ± 10.50 ###	91.91 ± 9.66	52.11 ± 5.57 *
Chol (mg/dL)	66.24 ± 4.265	26.78 ± 2.697 *	44.00 ± 4.856	110.2 ± 5.754 #	78.10 ± 3.247	53.67 ± 11.84 **

For the same cohort of animals as used in the current study, estimated daily intake of FF has been reported in [24]; concentrations of triglycerides (TG) and total cholesterol (Chol) in blood serum follow the data originally published in [22]. These data are reused here to provide context for the present analyses. The data are means ± SEM, 7–20 animals per group. *, $p < 0.05$, **, $p < 0.01$, vs. control animals of the same age; #, $p < 0.05$, ###, $p < 0.001$, in old vs. young control rats. Symbols: yC, oC, young and old control groups; y.1, y.5, o.1, o.5, young and old rats treated with 0.1% or 0.5% FF, respectively.

3.2. Manifestations of Oxidative Stress

Oxidative stress in cardiac muscle of young and old FF-treated rats was evaluated using two indicators: 8-hydroxydeoxyguanosine (8-OHdG) level for oxidative DNA damage (by ELISA) and 4-hydroxynonenal (4-HNE) immunoreactivity (by IHC) for lipid peroxidation.

8-OHdG levels did not differ between young and old control groups. In young rats, FF did not affect 8-OHdG levels relative to control. 8-OHdG concentration increased in 0.5% vs. 0.1% FF-treated groups, revealing dose-dependent variation (Figure 1a). In old rats, both FF doses increased 8-OHdG levels, indicating enhanced oxidative DNA damage (Figure 1a).

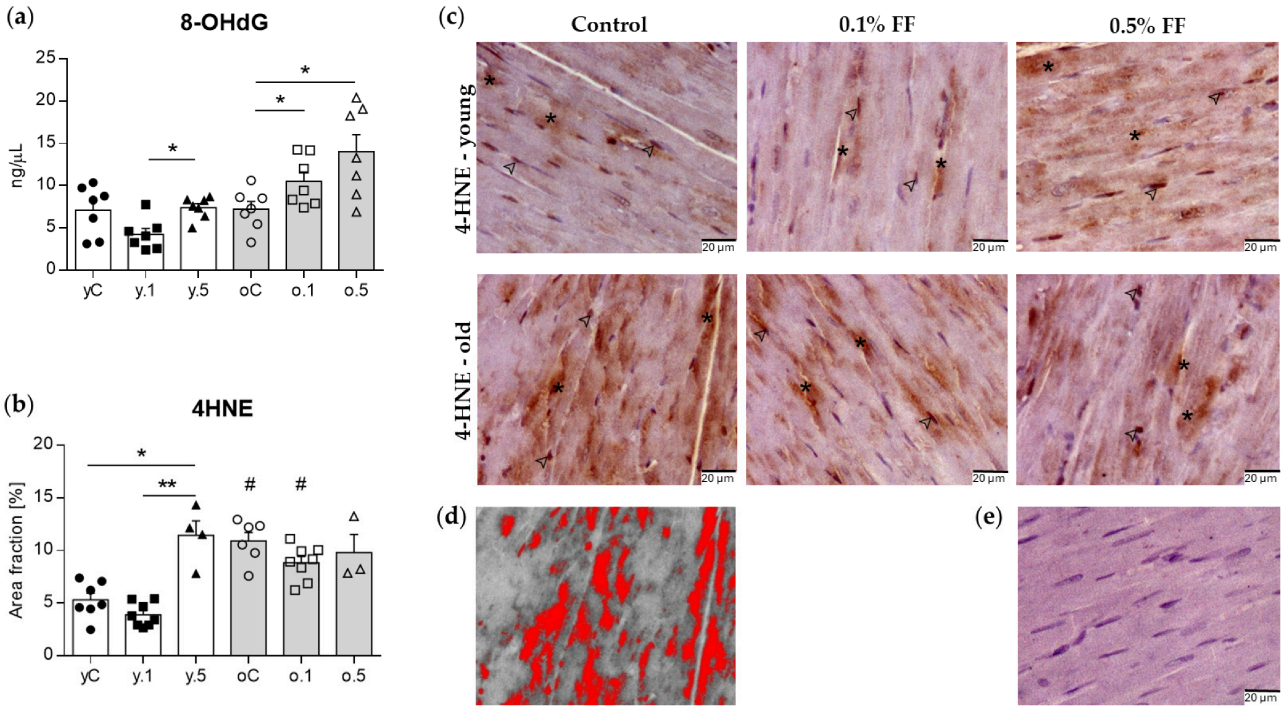

Figure 1. Fenofibrate affects cardiac oxidative stress indicators differently in young and old rats. (**a**) 8hy-droxydeoxyguanosine (8-OHdG) levels, measured by ELISA; means + SEM of 7 animals per group; * $p < 0.05$. (**b**) Quantification of 4-HNE immunoreactivity in sections of LV myocardium; means + SEM of 3–8 rats per group, averaged for at least 8 regions of interest (ROIs) per slide; * $p < 0.05$, ** $p < 0.01$; # $p < 0.05$ vs. respective young rat group. yC, oC, young and old control groups; y.1, y.5, o.1, o.5, young and old rats treated with 0.1% or 0.5% FF, respectively. (**c**) Representative microphotographs of 4-HNE-stained sections; arrowheads show examples of nuclear immunoreactivity, asterisks indicate areas with diffuse cytoplasmic immunoreactivity; scale bar 20 µm. (**d**) Example of semi-quantitative analysis of the microphotograph above (cellSens Dimension 4.1, Olympus Corp.). (**e**) Negative control.

4-HNE staining showed nuclear and diffuse cytoplasmic immunoreactivity (Ir) in cardiomyocytes of the left ventricle (LV) (Figure 1c). In controls, 4-HNE Ir was significantly higher in old than in young animals (Figure 1b). In young rats, low-dose FF had no effect, whereas high-dose FF increased 4-HNE Ir, suggesting enhanced lipid peroxidation. In old rats, neither FF dose significantly affected 4-HNE Ir (Figure 1b,c).

3.3. Fenofibrate-Induced Modulation of Antioxidant Response Effectors

The impact of FF on cardiac antioxidant response as a function of aging was analyzed by WB, IHC, and/or qPCR of key molecular targets. Basal levels of the studied proteins and transcripts were comparable between young and old controls, except for NAD(P)H quinone dehydrogenase 1 (Nqo1), whose protein level was higher in old rats (Figure 2a,b).

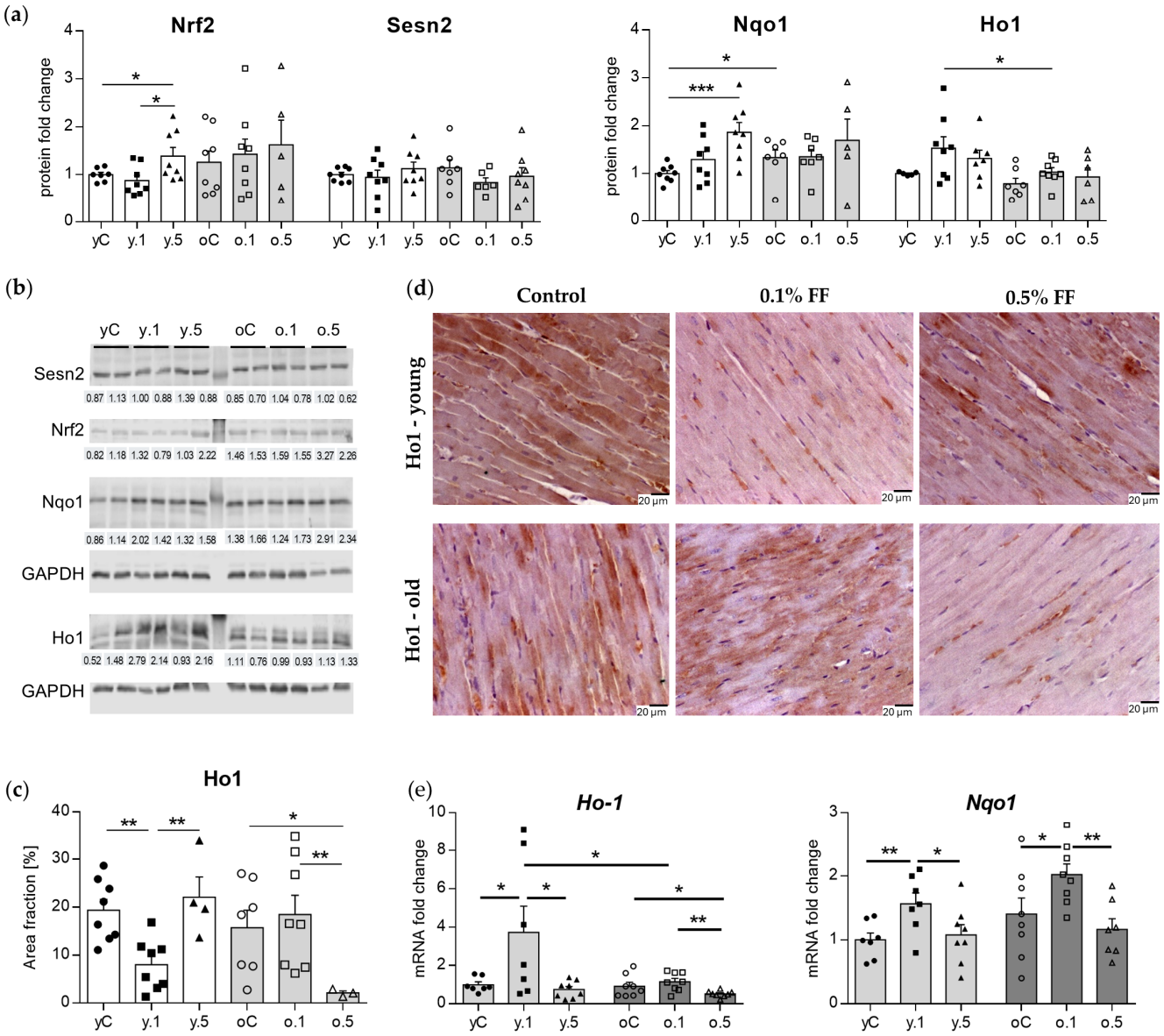

Figure 2. Fenofibrate-induced modulation of antioxidant response effectors in the heart. Young and old rats were treated per os with 0.1% FF (y.1, o.1) or 0.5% FF (y.5, o.5) for 30 days. (**a**) Protein expression of Nrf2, Sesn2, Nqo1, and Ho1, measured by immunoblotting; means + SEM of 5–8 animals per group; * $p < 0.05$, *** $p < 0.001$. (**b**) Representative blots with corresponding GAPDH loading controls. Values below the bands indicate densitometry intensity ratios relative to GAPDH. (**c**) Ho1 immunoreactivity in LV myocardium; means + SEM, at least 8 ROIs per slide, 4–8 rats per group; * $p < 0.05$, ** $p < 0.01$. (**d**) Representative microphotographs of Ho1-stained sections; scale bar 20 µm. (**e**) Gene expression of *Nqo1* and *Ho1*, measured by qPCR; means + SEM of 7–9 animals per group; * $p < 0.05$, ** $p < 0.01$. Western blot original images can be found in Figure S1.

In young rats, Nrf2 (nuclear factor erythroid 2-related factor 2), which controls the transcription of genes encoding cytoprotective enzymes, was not significantly affected by 0.1% FF, whereas 0.5% FF mildly upregulated Nrf2 protein levels relative to the control and 0.1% FF groups (Figure 2a). Sestrin 2 (Sesn2), which facilitates degradation of the repressor Keap1 and thereby enables Nrf2 activation, was unaffected. Among Nrf2 transcriptional targets, the protein levels of Nqo1 were significantly increased only after 0.5% FF, while those of heme oxygenase 1 (Ho1) did not change after either FF dose (Figure 2a).

In old rats, FF failed to produce a statistically significant induction of Nrf2 protein levels, which was accompanied by high inter-individual variability (Figure 2a). Likewise, Sesn2, Nqo1, and Ho1 protein levels were also unaffected by FF treatment. Thus, upregulation of Nrf2 protein and its downstream target Nqo in myocardium was restricted to young rats treated with high-dose FF.

Ho1 immunoreactivity, localized mainly in cardiomyocyte cytoplasm and fibrocytes/endothelial cells, showed a different pattern of changes. Basal Ho1 Ir was comparable between ages (Figure 2c,d). In young animals, 0.1% FF decreased Ho1 Ir, whereas 0.5% FF had no effect. In old rats, Ho1 Ir decreased after 0.5% FF, but not 0.1% FF (Figure 2c,d).

At the gene expression level, *Ho1* and *Nqo1* mRNA increased after 0.1% FF in young hearts, whereas 0.5% FF caused no changes (Figure 2e). In old rats, 0.1% FF increased *Nqo1*, while 0.5% FF had no effect. In aged hearts, neither dose increased *Ho1* expression, which was significantly lower than control after 0.5% FF (Figure 2e). Thus, low-dose FF exerted a stronger stimulatory effect on antioxidant gene expression than the high dose, with attenuated effects in old rats.

3.4. Fenofibrate Effects on Thiol-Based Redox-Active Proteins

Thiol-based redox-active proteins participate in maintaining cellular redox homeostasis and are transcriptionally regulated by Nrf2 [27]. In control rats, aging was associated with lower mRNA expression of sulfiredoxin 1 (*Srxn1*), peroxiredoxin 3 (*Prdx3*), and thioredoxin 1 (*Txn1*), but no changes in glutathione peroxidase 4 (*Gpx4*), *Prdx1*, *Prdx2*, *Prdx5*, and *Txn2* levels (Figure 3).

In young rats, 0.1% FF decreased *Gpx4* mRNA, whereas 0.5% FF had no effect. Neither dose affected *Srxn1*. Among peroxiredoxins, only *Prdx5* was upregulated, while *Prdx1*, *Prdx2*, and *Prdx3* remained unchanged. Mitochondrial *Txn2* increased after 0.5% FF, whereas predominantly cytoplasmic *Txn1* decreased (Figure 3).

In old rats, 0.1% FF reduced *Gpx4* and increased *Srxn1* expression, while 0.5% FF had no effect on either gene. Peroxiredoxins' mRNA levels were unaffected. *Txn2* was unchanged, whereas *Txn1* increased after 0.1% FF (Figure 3). Physiological aging therefore markedly altered the transcriptional response of thiol antioxidant defenses to fenofibrate, with young hearts showing predominantly mitochondrial antioxidant remodeling and aged hearts exhibiting a distinct, predominantly *Srxn1*/*Txn1*-related response.

3.5. Fenofibrate's Effects on the Expression of Angpt1 and eNOS

Angiopoietin 1 (Angpt1) and endothelial nitric oxide synthase (eNOS) contribute to cardiac antioxidant defenses by modulating vascular redox signaling and suppressing oxidative stress [28]. Angpt1 protein levels were lower in cardiac muscle of old rats than in young rats, whereas eNOS showed no significant age-related differences. In young animals, 0.5% FF increased Angpt1 expression, while no effect was observed in old rats. eNOS levels did not change with FF treatment (Figure 4). To conclude, physiological aging attenuated the fenofibrate-induced upregulation of the Angpt1 level observed in young hearts.

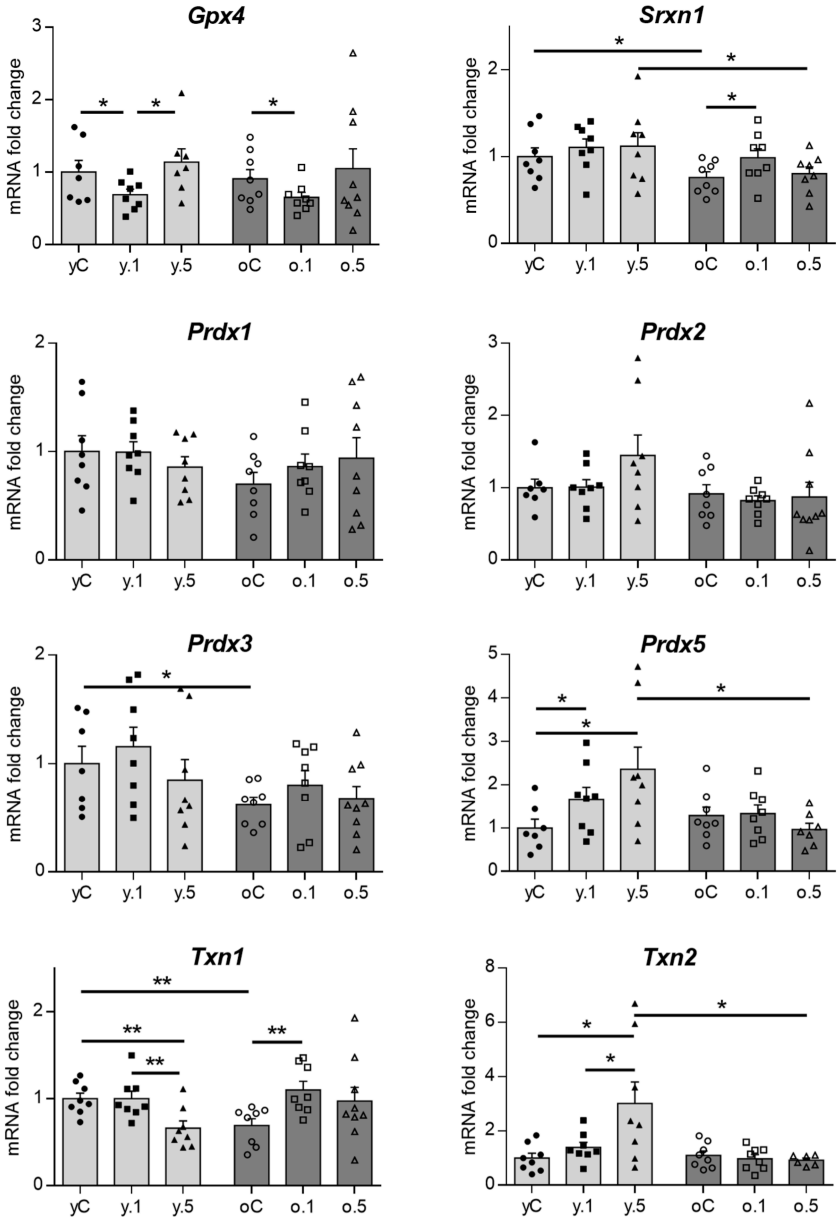

Figure 3. Fenofibrate modulates the gene expression of selected thiol antioxidant system enzymes in the hearts of young and old rats. Gene expression measured by qPCR and quantified relative to the young control group (yC = 1); means + SEM of 7–9 animals per group; * $p < 0.05$, ** $p < 0.01$.

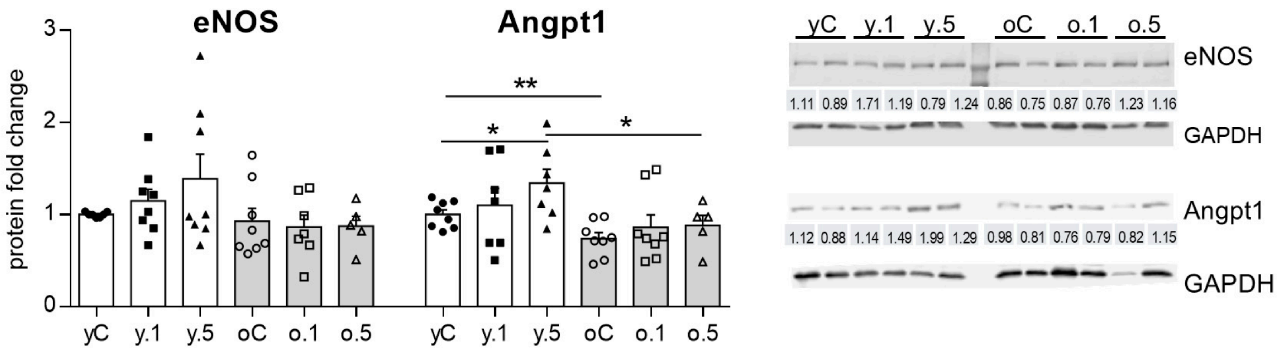

Figure 4. Effects of fenofibrate on eNOS and Angpt1 protein expression, measured by immunoblotting; means + SEM of 5–8 animals per group, normalized to young control group (yC = 1); * $p < 0.05$, ** $p < 0.01$. Representative blots are shown together with GAPDH loading control. Values below the

bands indicate densitometry intensity ratios relative to GAPDH. Western blot original images can be found in Figure S1.

The results obtained in this study are summarized in Table 3.

Table 3. Cardiac antioxidant responses to aging and fenofibrate treatment—summary of study results.

Target Marker	Assay Method & Sample Size	Basal Aging Effect (oC vs. yC)	Effect of FF in Young Rats	Effect of FF in Old Rats	Age × Treatment Effect
Oxidative Stress					
8-OHdG (DNA damage)	ELISA (n = 7)	No effect	No effect	↑ at 0.1% & 0.5% FF ($p < 0.05$)	$F(2, 36) = 4.29$, $p = 0.0214$
4-HNE (lipid peroxidation)	IHC (n = 3–8) 7/8/4/7/8/3 *	↑ in oC ($p < 0.01$)	↑ at 0.5% FF ($p < 0.05$)	No effect	$F(2,31) = 5.07$, $p = 0.0125$
Nrf2 & Antioxidant Enzymes					
Nrf2 protein	WB (n = 5–8) 7/8/8/8/8/5 *	No effect	↑ at 0.5% FF ($p < 0.05$)	No effect	No effect
Sesn2 protein	WB (n = 5–8) 7/8/8/8/8/5 *	No effect	No effect	No effect	No effect
Nqo1 protein	WB (n = 5–8) 8/8/8/7/7/5 *	↑ in oC ($p < 0.05$)	↑ at 0.5% FF ($p < 0.001$)	No effect	No effect
Nqo1 mRNA	qPCR (n = 7–8)	No effect	↑ at 0.1% FF ($p < 0.05$)	↑ at 0.1% FF ($p < 0.05$)	No effect
Ho1 protein	WB (n = 6–8) 6/8/7/7/8/6 *	No effect	No effect	No effect	No effect
Ho1 mRNA	qPCR (n = 7–8)	No effect	↑ at 0.1% FF ($p < 0.05$)	↓ at 0.5% FF ($p < 0.05$)	$F(2, 40) = 3.48$, $p = 0.0404$
Ho1 immunoreactivity	IHC (n = 3–8) 8/8/4/7/8/3 *	No effect	↓ at 0.1% FF ($p < 0.05$)	↓ at 0.5% FF ($p < 0.05$)	$F(2, 32) = 8.63$, $p = 0.0010$
Thiol-Based Redox-Active Proteins					
Gpx4 mRNA	qPCR (n = 7–8)	No effect	↓ at 0.1% FF ($p < 0.05$)	↓ at 0.1% FF ($p < 0.05$	No effect
Srxn1 mRNA	qPCR (n = 7–9)	↓ in oC ($p < 0.05$)	No effect	↑ at 0.1% FF ($p < 0.05$)	No effect
Prdx1, *Prdx2* mRNA	qPCR (n = 7–9)	No effect	No effect	No effect	No effect
Prdx3 mRNA	qPCR (n = 7–9)	↓ in oC ($p < 0.05$)	No effect	No effect	No effect
Prdx5 mRNA	qPCR (n = 7–9)	No effect	↑ at 0.1% & 0.5% FF ($p < 0.05$)	No effect	$F(2, 40) = 4.14$, $p = 0.0231$
Txn1 mRNA	qPCR (n = 7–9)	↓ in oC ($p < 0.05$)	↓ at 0.5% FF ($p < 0.05$)	↑ at 0.1% FF ($p < 0.05$)	$F(2, 43) = 4.62$, $p = 0.0153$
Txn2 mRNA	qPCR (n = 7–9)	No effect	↑ at 0.5% FF ($p < 0.05$)	No effect	$F(2, 40) = 4.53$, $p = 0.0168$
Vascular Axis					
Angpt1 protein	WB (n = 5–8) 8/7/7/8/8/5 *	↓ in oC ($p < 0.01$)	↑ at 0.1% FF ($p < 0.05$)	No effect	No effect
eNOS protein	WB (n = 5–8) 7/8/8/8/7/5 *	No effect	No effect	No effect	No effect

* For WB and IHC data, exact sample sizes are shown.

4. Discussion

The present study demonstrates that physiological aging is associated with a diminished antioxidant response to fenofibrate (FF) in the heart. In young rats, FF activated several components of antioxidant defense systems, yet these responses were blunted in old animals. Under basal conditions, aging differentially affected cardiac antioxidative systems, which appeared effective at the DNA-protection level but suppressed against lipid peroxidation. Responses to FF differed between young and old rat hearts. In young hearts, high-dose FF increased lipid peroxidation, evidenced by elevated 4-HNE immunoreactivity, whereas in aged hearts it substantially enhanced oxidative DNA injury. Our data indicate that physiological aging constrains FF-triggered antioxidant and redox defense pathways.

Oxidative stress arises from an imbalance between ROS generation and scavenging and is a hallmark of cardiac aging, contributing to progressive myocardial dysfunction [29]. 4-hydroxynonenal (4-HNE), a major product of lipid peroxidation, forms covalent adducts with proteins, modifying or inhibiting their functions [30]. Consistent with previous reports in rodents [31–33] and humans [34], 4-HNE immunoreactivity was elevated in old hearts, indicating increased lipid peroxidation. For the first time, we show age-related differences in cardiac response to FF under non-pathological conditions. Although FF reduces lipid peroxidation markers and restores the 4-HNE-detoxifying enzyme GPx4 in young rodents with septic cardiomyopathy [35], in our experiment, high-dose FF increased myocardial 4-HNE immunoreactivity in young rats, possibly indicating a maladaptive response to excessive FF stimulation. Indeed, moderate FF doses can improve fatty acid utilization and induce antioxidant genes through PPARα activation [16,36,37], whereas excessive PPARα activation increases β-oxidation and cardiac injury [38], potentially through enhanced ROS generation. In aged hearts, the lack of FF effect on 4-HNE immunoreactivity may reflect a ceiling effect in already oxidatively burdened tissue, reduced sensitivity to further measurable shifts, or changes masked by limited dynamic range.

Basal levels of 8-OHdG, a marker of oxidative DNA damage [39], did not differ between age groups, contrasting with increased genomic oxidative stress reported in aging human cardiomyocytes [40]. Under stress conditions, FF has been reported to reduce paraquat-induced 8-OHdG levels in cultured retinal/choroidal vascular endothelial cells [37]. However, in young rat myocardium, we did not detect any significant FF impact on 8-OHdG concentration. In aged hearts, both FF doses increased 8-OHdG, implying reduced capacity to buffer FF-induced oxidative challenges at the DNA level. Together, 4-HNE and 8-OHdG findings indicate that FF can be protective or pro-oxidant depending on dose and age, and that enhanced metabolic stimulation or advanced age may shift the balance between substrate oxidation and antioxidant buffering toward oxidative injury [24,25].

Nuclear factor erythroid 2-related factor 2 (Nrf2) regulates cellular antioxidant responses through transcriptional induction of antioxidant enzymes [41]. Antioxidative effects of FF via Nrf2 signaling have been demonstrated in cardiovascular disease models almost exclusively in young-adult animals [12,14,35]. We are the first to report age-related changes in rat hearts challenged with low and high FF doses. Our data indicate that FF-induced antioxidant stimulation functions in young myocardium but becomes impaired with age. Only in young rats did FF increase Nrf2 protein, accompanied by increased expression of Nqo1, a sensitive Nrf2 target. Aged hearts, while exhibiting high sample variance, lacked significant Nrf2 protein induction. Interestingly, old rats showed increased *Nqo1* mRNA but not protein after low-dose treatment. The mRNA–protein level discordances may reflect differences in mRNA stability, translation efficiency, and/or protein turnover [42–44]. We suggest that aging might reduce the capacity of FF to activate Nrf2-dependent transcription, consistent with age-related decline in Nrf2 signaling through enhanced Keap1-mediated repression, reduced antioxidant response element competence,

and epigenetic changes [34,45]. However, this hypothesis requires further testing for Nrf2 activity and with functional antioxidant assays.

Aging had no effect on cardiac protein levels or immunoreactivity of Ho1, consistent with previous findings in Wistar rats [46]. For the first time, we examined Ho1 responses to FF in the context of aging. While there were no significant changes in Ho1 protein abundance revealed by immunoblotting, IHC showed reduced myocardial Ho1 staining in young rats treated with 0.1% FF and old rats receiving 0.5% FF. These findings may indicate redistribution of Ho1 expression among cell populations of the cardiac tissue rather than a simple change in total protein content.

A notable finding is the age-dependent differential regulation by FF of the thiol-based antioxidant system at the transcriptional level. Peroxiredoxins (Prdxs) reduce hydrogen peroxide and organic hydroperoxides, thioredoxins (Txns) provide reducing equivalents for their regeneration, and sulfiredoxin (Srxn) restores overoxidized peroxiredoxins to their active form [27]. Glutathione peroxidase 4 (Gpx4), an essential antioxidant peroxidase localized to mitochondria, cytosol, and nucleus, acts in parallel with the thioredoxin system to maintain redox balance, protect membranes from lipid peroxidation, and regulate ferroptotic cell death [47,48]. These genes are regulated by Nrf2 [41] and, to some extent, by posttranslational modifications [19]. In control rats, aging was associated with lower *Srxn1*, *Prdx3*, and *Txn1* mRNA expression, consistent with loss of redox resilience during cardiac aging [19,48–50]. Prdx3 declines in intramyofibrillar mitochondria of the myocardium of 24-month-old mice [49] and in human failing myocardium [51], whereas no age-related changes have been reported for Prdx1, Prdx2, or Prdx5 expression [49]. Moreover, *Txn* expression decreases in the myocardium of old and senescent Wistar rats [19], supporting the conclusion that aging deteriorates the capacity to restore redox-active thiols.

Our results further show that aging differentially affects the response of cardiac redox-active proteins to FF. In young rats, FF treatment altered the expression profile of cardiac thiol redox genes, marked by increased mitochondrial *Txn2* and *Prdx5* mRNA alongside decreased *Gpx4* transcript levels, indicating a selective engagement of specific antioxidant components. Because Prdx5 and Txn2 are strongly involved in mitochondrial peroxide handling and redox homeostasis [27,49], their induction may reflect an adaptive response to increased fatty acid oxidation and mitochondrial oxidant production upon treatment with FF, a PPARα agonist. However, the concomitant reduction in *Gpx4* may increase susceptibility to membrane lipid oxidation [41], potentially explaining the increase in 4-HNE immunoreactivity after high-dose FF. Unlike our healthy aging model, in young mice with LPS-induced sepsis, cardiac Gpx4 protein was elevated by FF, while FF-treated controls showed no difference from untreated controls [35]. In retinal–choroidal vascular endothelial cells, FF upregulated Prdx1 and Trx2 expression under oxidative stress [37]. Overall, FF may strengthen mitochondrial peroxide detoxification while simultaneously reducing protection against lipid peroxidation in young hearts. However, unlike young animals, FF-induced changes in mitochondrial redox-active protein mRNA expression were largely absent in aged hearts. Low-dose FF mildly reduced *Gpx4* and modestly increased *Srxn1* and *Txn1*, whereas *Prdxs* and *Txn2* were unaffected, and high-dose FF produced no changes. Thus, FF can induce a predominantly mitochondrial antioxidant program in young myocardium, but this adaptive shift is constrained in aged hearts.

FF may influence cardiac redox homeostasis through vascular signaling. Angpt1 promotes endothelial stability, suppresses vascular inflammation [28], and enhances eNOS activation, increasing nitric oxide bioavailability [52]. Nitric oxide can limit oxidative stress by reducing leukocyte adhesion, improving microvascular perfusion, and modulating mitochondrial ROS production [53]. Lower basal Angpt1 in aged hearts is consistent with age-associated endothelial dysfunction [54]. High-dose FF increased Angpt1 only

in young rats, with no effect on eNOS levels. FF has been shown to increase eNOS expression and endothelial function in aortae of streptozotocin-induced diabetic mice [55], hearts of doxorubicin-induced cardiomyopathy mice [56], and rat cardiomyocyte models of hypoxia/reperfusion or high-glucose-induced injury, but not in control FF-treated cells [17]. Our findings suggest mild activation of Angpt1 by FF in young, but not old, rat hearts.

The findings of the present study should be interpreted alongside structural damage previously characterized in this same animal cohort, where, only in aged hearts, 0.5% FF induced fibrosis and highly elevated the hypertrophy marker NPPA, while 0.1% FF caused almost no structural changes in either age group [25]. In view of these data, the currently observed limited induction of antioxidant effectors in aged hearts seems to be a primary age-dependent molecular effect rather than a secondary consequence of tissue injury. In particular, high-dose FF in young rats induced Nrf2 and mitochondrial redox-active proteins (Txn2, Prdx5) within structurally normal myocardium [25]. However, with high FF exposure in aged hearts, antioxidant response impairment and structural remodeling possibly form a maladaptive feed-forward loop. Excessive PPARα-driven fatty acid oxidation overwhelms aged cardiomyocyte mitochondria [25,38], with accumulating ROS driving lipid peroxidation and DNA damage that contribute to pro-fibrotic cascades [57]. However, this interpretation requires further testing.

Our findings demonstrate that cardiac responses to FF do not follow a simple monotonic dose–response relationship. Instead, the effects reflect a delicate balance between moderate adaptive stimulation and high-dose metabolic burden. Low-dose FF (0.1%; ~42–52 mg/kg/day) exerted subtle, protective transcriptional responses without elevating markers of lipid peroxidation or oxidative DNA damage. Conversely, high-dose FF (0.5%; ~210–260 mg/kg/day), while required to induce Nrf2 protein and the gene expression of mitochondrially located Txn2/Prdx5 in young hearts, also unmasked cardiac lipid peroxidation (4-HNE) in young animals and oxidative DNA damage (8-OHdG) in old rats, possibly through induction of oxidative metabolism [25]. These findings indicate that higher FF exposure can exceed the antioxidant buffering capacity of aged myocardium, shifting the drug's profile from an adaptive stimulus to a pro-oxidant challenge. Further studies in oxidative stress models are needed to elucidate how aging limits the heart's capacity to engage FF-responsive cytoprotective networks.

To contextualize the translational relevance of our experimental design, the 30-day timeframe (comparable to, e.g., [12,38]) was chosen as a period capable of eliciting steady-state changes at the cell and organ levels, while avoiding age-related mortality in old rats. The comparative-aging literature indicates that 30 days in adult rats correspond to approximately 2.5 to 3 human years [58], mimicking chronic FF therapy in patients. Because rodents possess an accelerated basal metabolic rate and faster protein turnover, drug-induced metabolic and structural remodeling manifest more quickly than the year-equivalent period in humans. Therefore, the 30-day period in our rat model captures relatively long-term outcomes of FF treatment.

Several limitations should be considered. First, transcript and/or protein measurements provide molecular clues but do not directly reflect functional antioxidant response, e.g., through Nrf2 signaling. The protein abundance of the Nrf2 repressor Keap1 was not quantified, and Nrf2 was evaluated in whole-cell lysates without nuclear fractionation or ARE-binding assays. Furthermore, downstream Nrf2 effectors can also be regulated by alternative pathways, including transcriptional activation of *Ho1* by PPARα ligands [59]. Further studies are needed to establish a mechanistic basis for the FF-induced response observed in our study.

Second, although cardiomyocytes represent almost 97% of heart volume/mass, bulk cardiac tissue does not distinguish the roles of fibrocytes/fibroblasts, endothelial cells, and immune cells.

Third, no a priori statistical power calculations were performed to determine sample sizes, which were based on published rodent experimental protocols. Consequently, the relatively small sample sizes in our study could have limited the statistical power to detect subtle treatment or ageing effects. Some potentially significant effects may have escaped statistical detection, which is particularly relevant when investigating aging, characterized by substantial inter-individual heterogeneity.

Lastly, only male rats were used; thus, our results might not extrapolate to females. Indeed, sex and gender are known to affect cardiovascular physiology as well as risk, presentation, and response to treatment of CVDs [60]. Importantly, differential sex-associated changes in transcription mediated by PPARα have been suggested to underlie sex-specific differences in mitochondrial oxidative capacity in failing mouse hearts [61]. Similarly, the magnitude of the response to FF may differ between sexes, which should be explored in future studies.

Despite these limitations, the study has important implications. Physiological aging appears to be a major determinant of FF responsiveness in the heart and may limit the therapeutic value of fibrates as an antioxidant strategy, beyond their lipid-lowering effects, in older individuals. Additional studies are needed to determine whether FF-associated changes translate into functional cardioprotection or long-term preservation of cardiac performance in humans.

5. Conclusions

In summary, fenofibrate induced limited antioxidant responses in the heart of young rats, characterized by selective activation of Nrf2-related genes, remodeling of thiol-based defenses toward mitochondrial antioxidants, and probable engagement of Angpt1-related signaling. Physiological aging weakened these responses and was associated with higher basal oxidative burden, reduced antioxidant reserve, and loss of fenofibrate inducibility. The data therefore support the view that age is a major determinant of fenofibrate's antioxidant effects in the heart.

Supplementary Materials: The following supporting information can be downloaded at https://www.mdpi.com/article/10.3390/biom16121715/s1: Figure S1: original blots.

Author Contributions: Conceptualization, A.W.; formal analysis, A.W.; funding acquisition, A.W.; investigation, A.W. and J.K.; methodology, A.W. and J.K.; supervision, Z.K.; visualization, A.W.; writing—original draft preparation, A.W. and Z.K.; writing—review and editing, A.W., J.K., and Z.K. All authors have read and agreed to the published version of the manuscript.

Funding: This research was financed by the Polish Ministry of Science and Higher Education program 'Excellence Initiative—Research University', in the form of an individual researcher grant from the Medical University of Gdańsk to A.W. (71-01422/K10-0007236/61/280/280/2024).

Institutional Review Board Statement: The animal study protocol was approved by the Local Ethical Committee in Bydgoszcz, Poland (protocols Nos. 41/2017, 58/2017, 40/2018, and 5/2019, approved on 27 July 2017, 23 November 2017, 16 October 2018, and 20 February 2019, respectively).

Data Availability Statement: The original contributions presented in this study are included in the article and Supplementary Materials. Further inquiries can be directed to the corresponding author.

Acknowledgments: During the preparation of this manuscript, the authors used ChatGPT-5.6 for language polishing in some parts of the manuscript. The authors reviewed and edited the output and take full responsibility for the content of the published article.

Conflicts of Interest: The authors declare no conflicts of interest.

References

1. Chong, B.; Jayabaskaran, J.; Jauhari, S.M.; Chan, S.P.; Goh, R.; Kueh, M.T.W.; Li, H.; Chin, Y.H.; Kong, G.; Anand, V.V.; et al. Global burden of cardiovascular diseases: Projections from 2025 to 2050. *Eur. J. Prev. Cardiol.* **2024**, *32*, 1001–1015. [CrossRef] [PubMed]
2. Mubarik, S.; Naeem, S.; Shen, H.; Mubarak, R.; Luo, L.; Hussain, S.R.; Hak, E.; Yu, C.; Liu, X. Population-Level Distribution, Risk Factors, and Burden of Mortality and Disability-Adjusted Life Years Attributable to Major Noncommunicable Diseases in Western Europe (1990–2021): Ecological Analysis. *JMIR Public Health Surveill.* **2024**, *10*, e57840. [CrossRef] [PubMed]
3. Sidhu, G.; Tripp, J. Fenofibrate. In *StatPearls*; StatPearls Publishing: Treasure Island, FL, USA, 2023.
4. The ACCORD Study Group; Ginsberg, H.N.; Elam, M.B.; Lovato, L.C.; Crouse, J.R., 3rd; Leiter, L.A.; Linz, P.; Friede-Wald, W.T.; Buse, J.B.; Gerstein, H.C.; et al. Effects of combination lipid therapy in type 2 diabetes mellitus. *N. Engl. J. Med.* **2010**, *362*, 1563–1574. [CrossRef] [PubMed]
5. Jo, S.H.; Nam, H.; Lee, J.; Park, S.; Lee, J.; Kyoung, D.S. Fenofibrate Use Is Associated With Lower Mortality and Fewer Cardiovascular Events in Patients With Diabetes: Results of 10,114 Patients From the Korean National Health Insurance Service Cohort. *Diabetes Care* **2021**, *44*, 1868–1876. [CrossRef] [PubMed]
6. Keech, A.; Simes, R.J.; Barter, P.; Best, J.; Scott, R.; Taskinen, M.R.; Forder, P.; Pillai, A.; Davis, T.; Glasziou, P.; et al. Effects of long-term fenofibrate therapy on cardiovascular events in 9795 people with type 2 diabetes mellitus (the FIELD study): Randomised controlled trial. *Lancet* **2005**, *366*, 1849–1861. [CrossRef] [PubMed]
7. Kim, S.K.; Zhao, Z.S.; Lee, Y.J.; Lee, K.E.; Kang, S.M.; Choi, D.; Lim, S.; Chung, N.; Lee, H.C.; Cha, B.S. Left-ventricular diastolic dysfunction may be prevented by chronic treatment with PPAR-alpha or -gamma agonists in a type 2 diabetic animal model. *Diabetes Metab. Res. Rev.* **2003**, *19*, 487–493. [CrossRef] [PubMed]
8. Park, J.; Song, H.; Moon, S.; Kim, Y.; Cho, S.; Han, K.; Park, C.-Y.; Cho, S.W.; Oh, C.-M. Cardiometabolic benefits of fenofibrate in heart failure related to obesity and diabetes. *Cardiovasc. Diabetol.* **2024**, *23*, 343. [CrossRef] [PubMed]
9. Yeh, C.H.; Chen, T.P.; Lee, C.H.; Wu, Y.C.; Lin, Y.M.; Lin, P.J. Cardiomyocytic apoptosis following global cardiac ischemia and reperfusion can be attenuated by peroxisome proliferator-activated receptor alpha but not gamma activators. *Shock* **2006**, *26*, 262–270. [CrossRef] [PubMed]
10. Yue, T.L.; Bao, W.; Jucker, B.M.; Gu, J.L.; Romanic, A.M.; Brown, P.J.; Cui, J.; Thudium, D.T.; Boyce, R.; Burns-Kurtis, C.L.; et al. Activation of peroxisome proliferator-activated receptor-alpha protects the heart from ischemia/reperfusion injury. *Circulation* **2003**, *108*, 2393–2399. [CrossRef] [PubMed]
11. Althurwi, H.N.; Elshenawy, O.H.; El-Kadi, A.O.S. Fenofibrate modulates cytochrome P450 and arachidonic acid metabolism in the heart and protects against isoproterenol-induced cardiac hypertrophy. *J. Cardiovasc. Pharmacol.* **2014**, *63*, 167–177. [CrossRef] [PubMed]
12. Castiglioni, L.; Pignieri, A.; Fiaschè, M.; Giudici, M.; Crestani, M.; Mitro, N.; Abbate, M.; Zoja, C.; Rottoli, D.; Foray, C.; et al. Fenofibrate attenuates cardiac and renal alterations in young salt-loaded spontaneously hypertensive stroke-prone rats through mitochondrial protection. *J. Hypertens.* **2018**, *36*, 1129–1146. [CrossRef] [PubMed]
13. Lebrasseur, N.K.; Duhaney, T.A.S.; De Silva, D.S.; Cui, L.; Ip, P.C.; Joseph, L.; Sam, F. Effects of fenofibrate on cardiac remodeling in aldosterone-induced hypertension. *Hypertension* **2007**, *50*, 489–496. [CrossRef] [PubMed]
14. Zeng, S.Y.; Lu, H.Q.; Yan, Q.J.; Zou, J. A Reduction in ADAM17 Expression Is Involved in the Protective Effect of the PPAR-α Activator Fenofibrate on Pressure Overload-Induced Cardiac Hypertrophy. *PPAR Res.* **2018**, *2018*, 7916953. [CrossRef] [PubMed]
15. Malur, P.; Menezes, A.; DiNicolantonio, J.J.; O'Keefe, J.H.; Lavie, C.J. The Microvascular and Macrovascular Benefits of Fibrates in Diabetes and the Metabolic Syndrome: A review. *Mo. Med.* **2017**, *114*, 464–471. [PubMed]
16. Ibarra-Lara, L.; Sánchez-Aguilar, M.; Sánchez-Mendoza, A.; Del Valle-Mondragón, L.; Soria-Castro, E.; Carreón-Torres, E.; Díaz-Díaz, E.; Vázquez-Meza, H.; Guarner-Lans, V.; Rubio-Ruiz, M.E. Fenofibrate Therapy Restores Antioxidant Protection and Improves Myocardial Insulin Resistance in a Rat Model of Metabolic Syndrome and Myocardial Ischemia: The Role of Angiotensin II. *Molecules* **2016**, *22*, 31. [CrossRef] [PubMed]
17. Cortes-Lopez, F.; Sanchez-Mendoza, A.; Centurion, D.; Cervantes-Perez, L.G.; Castrejon-Tellez, V.; Del Valle-Mondragon, L.; Soria-Castro, E.; Ramirez, V.; Sanchez-Lopez, A.; Pastelin-Hernandez, G.; et al. Fenofibrate Protects Cardiomyocytes from Hypoxia/Reperfusion- and High Glucose-Induced Detrimental Effects. *PPAR Res.* **2021**, *2021*, 8895376. [CrossRef] [PubMed]
18. Zhang, J.; Cheng, Y.; Gu, J.; Wang, S.; Zhou, S.; Wang, Y.; Tan, Y.; Feng, W.; Fu, Y.; Mellen, N.; et al. Fenofibrate increases cardiac autophagy via FGF21/SIRT1 and prevents fibrosis and inflammation in the hearts of Type 1 diabetic mice. *Clin. Sci.* **2016**, *130*, 625–641. [CrossRef] [PubMed]
19. Kaplán, P.; Tatarková, Z.; Lichardusová, L.; Kmeťová Sivoňová, M.; Tomašcová, A.; Račay, P.; Lehotský, J. Age-Associated Changes in Antioxidants and Redox Proteins of Rat Heart. *Physiol. Res.* **2019**, *68*, 883–892. [CrossRef] [PubMed]

20. Li, Q.; Jiang, Y.; Song, A.; Li, Y.; Xu, X.; Xu, R. The Association Between Chronological Age and Dyslipidemia: A Cross-Sectional Study in Chinese Aged Population. *Clin. Interv. Aging* **2023**, *18*, 667–675. [CrossRef] [PubMed]
21. Andres, T.M.; McGrane, T.; McEvoy, M.D.; Allen, B.F.S. Geriatric Pharmacology: An Update. *Anesth. Clin.* **2019**, *37*, 475–492. [CrossRef] [PubMed]
22. Zubrzycki, A.; Wrońska, A.; Kotulak-Chrząszcz, A.; Wierzbicki, P.M.; Kmieć, Z. Fenofibrate impairs liver function and structure more pronounced in old than young rats. *Arch. Gerontol. Geriatr.* **2020**, *91*, 104244. [CrossRef] [PubMed]
23. Wronska, A.; Zubrzycki, A.; Kotlarz, G.; Kmiec, Z. Fenofibrate mildly stimulates browning-associated expression in white adipose tissues of young but not old male rats. *J. Physiol. Pharmacol.* **2023**, *74*, 169–183. [CrossRef] [PubMed]
24. Wrońska, A.; Kieżun, J.; Kmieć, Z. High-Dose Fenofibrate Stimulates Multiple Cellular Stress Pathways in the Kidney of Old Rats. *Int. J. Mol. Sci.* **2024**, *25*, 3038. [CrossRef] [PubMed]
25. Wrońska, A.; Kieżun, J.; Kmieć, Z. Fenofibrate Differently Affects the Heart's Morphology and Metabolism in Young and Old Rats. *Int. J. Mol. Sci.* **2025**, *26*, 8038. [CrossRef] [PubMed]
26. Kiezun, J.; Godlewski, J.; Krazinski, B.E.; Kozielec, Z.; Kmiec, Z. Galanin Receptors (GalR1, GalR2, and GalR3) Expression in Colorectal Cancer Tissue and Correlations to the Overall Survival and Poor Prognosis of CRC Patients. *Int. J. Mol. Sci.* **2022**, *23*, 3735. [CrossRef] [PubMed]
27. Andreadou, I.; Efentakis, P.; Frenis, K.; Daiber, A.; Schulz, R. Thiol-based redox-active proteins as cardioprotective therapeutic agents in cardiovascular diseases. *Basic. Res. Cardiol.* **2021**, *116*, 44. [CrossRef] [PubMed]
28. Parikh, S.M. Angiopoietins and Tie2 in vascular inflammation. *Curr. Opin. Hematol.* **2017**, *224*, 432–438. [CrossRef] [PubMed]
29. Pagan, L.U.; Gomes, M.J.; Gatto, M.; Mota, G.A.F.; Okoshi, K.; Okoshi, M.P. The Role of Oxidative Stress in the Aging Heart. *Antioxidants* **2022**, *11*, 336. [CrossRef] [PubMed]
30. Ayala, A.; Muñoz, M.F.; Argüelles, S. Lipid peroxidation: Production, metabolism, and signaling mechanisms of malondialdehyde and 4-hydroxy-2-nonenal. *Oxid. Med. Cell. Longev.* **2014**, *2014*, 360438. [CrossRef] [PubMed]
31. Fannin, J.; Rice, K.M.; Thulluri, S.; Arvapalli, R.K.; Wehner, P.; Blough, E.R. The Effects of Aging on Indices of Oxidative Stress and Apoptosis in the Female Fischer 344/Nnia X Brown Norway/BiNia Rat Heart. *Open Cardiovasc. Med. J.* **2013**, *7*, 113–121. [CrossRef] [PubMed]
32. Muthu, S.; Tran, Z.; Thilagavathi, J.; Bolarum, T.; Azzam, E.I.; Suzuki, C.K.; Sundararajan, V. Aging triggers mitochondrial, endoplasmic reticulum, and metabolic stress responses in the heart. *J. Cardiovasc. Aging* **2025**, *5*, 4. [CrossRef] [PubMed]
33. Tatarková, Z.; Kuka, S.; Račay, P.; Lehotský, J.; Dobrota, D.; Mištuna, D.; Kaplán, P. Effects of aging on activities of mitochondrial electron transport chain complexes and oxidative damage in rat heart. *Physiol. Res.* **2011**, *60*, 281–289. [CrossRef] [PubMed]
34. Rizvi, F.; Preston, C.C.; Emelyanova, L.; Yousufuddin, M.; Viqar, M.; Dakwar, O.; Ross, G.R.; Faustino, R.S.; Holmuhamedov, E.L.; Jahangir, A. Effects of Aging on Cardiac Oxidative Stress and Transcriptional Changes in Pathways of Reactive Oxygen Species Generation and Clearance. *J. Am. Heart Assoc.* **2021**, *10*, e019948. [CrossRef] [PubMed]
35. Chen, M.; Ma, P.; Liang, J.; Zhu, S.; Ren, J. Fenofibrate ameliorates LPS-induced cardiac injury through alleviation of ferroptosis. *Immunopharmacol. Immunotoxicol.* **2025**, *47*, 508–516. [CrossRef] [PubMed]
36. Castiglioni, L.; Gelosa, P.; Muluhie, M.; Mercuriali, B.; Rzemieniec, J.; Gotti, M.; Fiordaliso, F.; Busca, G.; Sironi, L. Fenofibrate reduces cardiac remodeling by mitochondrial dynamics preservation in a renovascular model of cardiac hypertrophy. *Eur. J. Pharmacol.* **2024**, *978*, 176767. [CrossRef] [PubMed]
37. Hsu, Y.J.; Lin, C.W.; Cho, S.L.; Yang, W.S.; Yang, C.M.; Yang, C.H. Protective Effect of Fenofibrate on Oxidative Stress-Induced Apoptosis in Retinal-Choroidal Vascular Endothelial Cells: Implication for Diabetic Retinopathy Treatment. *Antioxidants* **2020**, *9*, 712. [CrossRef] [PubMed]
38. Pettersen, J.C.; Pruimboom-Brees, I.; Francone, O.L.; Amacher, D.E.; Boldt, S.E.; Kerlin, R.L.; Ballinger, W.E. The PPAR alpha agonists fenofibrate and CP-778875 cause increased beta-oxidation, leading to oxidative injury in skeletal and cardiac muscle in the rat. *Toxicol. Pathol.* **2012**, *40*, 435–447. [CrossRef] [PubMed]
39. Li, Y.; Wang, X. The role of DNA and RNA guanosine oxidation in cardiovascular diseases. *Pharmacol. Res.* **2024**, *204*, 107187. [CrossRef] [PubMed]
40. Choudhury, S.; Huang, A.Y.; Kim, J.; Zhou, Z.; Morillo, K.; Maury, E.A.; Tsai, J.W.; Miller, M.B.; Lodato, M.A.; Araten, S.; et al. Somatic mutations in single human cardiomyocytes reveal age-associated DNA damage and widespread oxidative genotoxicity. *Nat. Aging* **2022**, *2*, 714–725. [CrossRef] [PubMed]
41. Chen, Q.M.; Maltagliati, A.J. Nrf2 at the heart of oxidative stress and cardiac protection. *Physiol. Genom.* **2018**, *50*, 77–97. [CrossRef] [PubMed]
42. Liu, Y.; Beyer, A.; Aebersold, R. On the Dependency of Cellular Protein Levels on mRNA Abundance. *Cell* **2016**, *165*, 535–550. [CrossRef] [PubMed]
43. Woodward, K.; Shirokikh, N.E. Translational control in cell ageing: An update. *Biochem. Soc. Trans.* **2021**, *49*, 2853–2869. [CrossRef] [PubMed]

44. Wu, X.; Wei, J.; Yi, Y.; Gong, Q.; Gao, J. Activation of Nrf2 signaling: A key molecular mechanism of protection against cardiovascular diseases by natural products. *Front. Pharmacol.* **2022**, *13*, 1057918. [CrossRef] [PubMed]
45. Bernatoniene, J.; Kopustinskiene, D.M.; Casale, R.; Medoro, A.; Davinelli, S.; Saso, L.; Petrikonis, K. Nrf2 Modulation by Natural Compounds in Aging, Neurodegeneration, and Neuropathic Pain. *Pharmaceutics* **2026**, *18*, 118. [CrossRef] [PubMed]
46. Qian, X.; Asad, S.B.; Li, J.; Wang, J.; Wei, D.; Zhao, Y.; Wang, Y.; Zhu, H. Link between cardiac function and the antioxidative defense mechanism in aged rats. *Biochem. Biophys. Res. Commun.* **2019**, *513*, 1100–1105. [CrossRef] [PubMed]
47. Dey, S.; Sidor, A.; O'Rourke, B. Compartment-specific Control of Reactive Oxygen Species Scavenging by Antioxidant Pathway Enzymes. *J. Biol. Chem.* **2016**, *291*, 11185–11197. [CrossRef] [PubMed]
48. Xiong, X.; Wang, G.; Wang, Y.; Zhang, T.; Bao, Y.; Wang, K.; Ainiwaer, D.; Sun, Z. Klotho protects against aged myocardial cells by attenuating ferroptosis. *Exp. Gerontol.* **2023**, *175*, 112157. [CrossRef] [PubMed]
49. Chen, Q.; Thompson, J.; Hu, Y.; Lesnefsky, E.J. Endoplasmic reticulum stress and alterations of peroxiredoxins in aged hearts. *Mech. Ageing Dev.* **2023**, *215*, 111859. [CrossRef] [PubMed]
50. Cui, C.; Song, H.; Guo, Y.; Shi, J.; Geng, B.; Wang, G. The Nrf Family and Its Cardioprotective Potential: Mechanisms, Functions, and Therapeutic Perspectives. *Drug Des. Dev. Ther.* **2025**, *19*, 8339–8373. [CrossRef] [PubMed]
51. Brixius, K.; Schwinger, R.H.G.; Hoyer, F.; Napp, A.; Renner, R.; Bölck, B.; Kümin, A.; Fischer, U.; Mehlhorn, U.; Werner, S.; et al. Isoform-specific downregulation of peroxiredoxin in human failing myocardium. *Life Sci.* **2007**, *81*, 823–831. [CrossRef] [PubMed]
52. Alfieri, A.; Ong, A.C.M.; Kammerer, R.A.; Solanky, T.; Bate, S.; Tasab, M.; Brown, N.J.; Brookes, Z.L. Angiopoietin-1 regulates microvascular reactivity and protects the microcirculation during acute endothelial dysfunction: Role of eNOS and VE-cadherin. *Pharmacol. Res.* **2014**, *80*, 43–51. [CrossRef] [PubMed]
53. Lin, X.; Zhang, Y.; Pu, J.; Peng, Y. Targeting muscle-vasculature crosstalk in aging through the integrative roles of L-citrulline, leucine, and exercise: Focus on muscle metabolism, vascular function, and sarcopenia prevention. *Front. Nutr.* **2025**, *12*, 1739173. [CrossRef] [PubMed]
54. Alvarez de Sotomayor, M.; Mingorance, C.; Andriantsitohaina, R. Fenofibrate improves age-related endothelial dysfunction in rat resistance arteries. *Atherosclerosis* **2007**, *193*, 112–120. [CrossRef] [PubMed]
55. Xin, R.; An, D.; Li, Y.; Fu, J.; Huang, F.; Zhu, Q. Fenofibrate improves vascular endothelial function in diabetic mice. *Biomed. Pharmacother.* **2019**, *112*, 108722. [CrossRef] [PubMed]
56. Huang, W.P.; Yin, W.H.; Chen, J.S.; Huang, P.H.; Chen, J.W.; Lin, S.J. Fenofibrate attenuates doxorubicin-induced cardiac dysfunction in mice via activating the eNOS/EPC pathway. *Sci. Rep.* **2021**, *11*, 1159. [CrossRef] [PubMed]
57. Liu, R.M.; Gaston Pravia, K.A. Oxidative stress and glutathione in TGF-beta-mediated fibrogenesis. *Free Radic. Biol. Med.* **2010**, *48*, 1–15. [CrossRef] [PubMed]
58. Sengupta, P. The Laboratory Rat: Relating Its Age with Human's. *Int. J. Prev. Med.* **2013**, *4*, 624–630. [PubMed]
59. Krönke, G.; Kadl, A.; Ikonomu, E.; Blüml, S.; Fürnkranz, A.; Sarembock, I.J.; Bochkov, V.N.; Exner, M.; Binder, B.R.; Leitinger, N. Expression of heme oxygenase-1 in human vascular cells is regulated by peroxisome proliferator-activated receptors. *Arter. Thromb. Vasc. Biol.* **2013**, *27*, 1276–1282. [CrossRef] [PubMed]
60. Clayton, J.A.; Gaugh, M.D. Sex as a Biological Variable in Cardiovascular Diseases: JACC Focus Seminar 1/7. *J. Am. Coll. Cardiol.* **2022**, *79*, 1388–1397. [CrossRef] [PubMed]
61. Ritterhoff, J.; McMillen, T.S.; Villet, O.; Young, S.; Kolwicz, S.C., Jr.; Senn, T.; Caudal, A.; Tian, R. Increasing fatty acid oxidation elicits a sex-dependent response in failing mouse hearts. *J. Mol. Cell. Cardiol.* **2021**, *158*, 1–10. [CrossRef] [PubMed]

Disclaimer/Publisher's Note: The statements, opinions and data contained in all publications are solely those of the individual author(s) and contributor(s) and not of MDPI and/or the editor(s). MDPI and/or the editor(s) disclaim responsibility for any injury to people or property resulting from any ideas, methods, instructions or products referred to in the content.